EPSC Abstracts
Vol. 8, EPSC2013-439-1, 2013
European Planetary Science Congress 2013

Dependence of O^+ escape rate from the Venusian upper atmosphere on IMF directions

K. Masunaga (1,2), Y. Futaana (2) and G. Stenberg (2), S. Barabash (2), T. L. Zhang (3), A. Fedorov (4), S. Okano (5), and N. Terada (1)

(1) Department of Geophysics, Graduate School of Science, Tohoku University, Sendai, Japan, (2) Swedish Institute of Space Physics, Kiruna, Sweden, (3) Space Research Institute, Austrian Academy of Science, Graz, Austria, (4) Centre d'Etude Spatiale des Rayonnements, Toulouse, France, (5) Institute for Astronomy, University of Hawaii, Pukalani, HI, USA, (masu-kei@pat.gp.tohoku.ac.jp / Fax: +81-22-795-6537)

Abstract

We investigate the dependence of the O^+ escape rate from the Venusian upper atmosphere on the upstream interplanetary magnetic field (IMF) direction. Using the data obtained from the Analyser of Space Plasma and Energetic Atoms (ASPERA-4) instrument and the magnetometer (MAG) onboard Venus Express, O^+ fluxes observed in the night side region is statistically calculated. The data is classified into two cases: the perpendicular IMF case and the parallel IMF case, where IMF is nearly perpendicular to the solar wind velocity and nearly parallel to it. In the period between June 21 2006 and May 31, 2010, the O^+ escape rates of $(5.8 \pm 2.9) \times 10^{24}$ s^{-1} (perpendicular IMF case) and $(4.9 \pm 2.2) \times 10^{24}$ s^{-1} (parallel IMF case) are obtained. Since these values are not significantly different, we conclude that the IMF direction does not affect the total amount of O+ outflow from Venus. Several acceleration mechanisms must balance each other in order to keep the escape rate constant.

1. Introduction

Due to the lack of an intrinsic magnetic field at Venus, its upper atmosphere is directly exposed to the solar wind. The interplanetary magnetic field (IMF) embedded in the solar wind drapes around the ionosphere and creates an induced magnetosphere [*Zhang et al*., 2007]. The solar wind reaches down to the top of the ionosphere and erodes the ionospheric ions into space. The main escaping component is O^+ ions, which is the main constituent of the upper ionosphere of Venus [*Taylor et al*., 1980].

It is known that the O^+ escape flux at Venus depends strongly on solar wind's conditions such as corotational interaction regions (CIRs), coronal mass ejections (CMEs), and solar energetic particles (SEPs) [*Luhmann et al*., 2008; *Edberg et al*., 2011; *Futaana et al*., 2008].

Recently, the disappearing induced magnetosphere was observed when the IMF direction becomes parallel to the velocity vector of the solar wind [*Zhang et al., 2009*]. The IMF direction is one possible parameter to control atmospheric erosion from Venus since *Masunaga et al*. [2011] showed that the parallel condition produces multiple O^+ outflow channels because of the complicated IMF draping pattern.

In this study we calculate the O^+ escape rates at Venus during two different IMF configurations, parallel and perpendicular.

2. Instruments and Data selection

To calculate O^+ escape fluxes at Venus, we use two instruments onboard Venus Express (VEX): The Ion Mass Analyzer (IMA), which is a part of Analyzer of Space Plasma and Energetic Atoms (ASPERA-4) [*Barabash et al*., 2007a] instrument, and the magnetometer (MAG) [*Zhang et al*., 2006]. IMA measures ions with mass separation. The energy range is 0.01-36 keV/q with an energy resolution $\Delta E/E=0.07$. Its field of view is 360°×90° with a resolution 22.5°×10°. The time resolution for a full 3D ion velocity distribution is 192s. MAG provides all three components of the magnetic field vector, B_X, B_Y, and B_Z in the Venus Solar Orbital (VSO) frame (x points to the Sun, y to the opposite direction of the planetary motion, and z completes the right-hand system). We use the 4-s resolution data product of MAG. Using MAG data, we can convert the VSO frame into the Venus Solar Electric (VSE) frame (x points to the Sun, z along the convection electric field, and y completes the right-hand system). The convection electric field is $\mathbf{E_{SW}} = -\mathbf{V_{SW}} \times \mathbf{B_{SW}}$, where

$\mathbf{V_{SW}}$ is the solar wind velocity (which we assume is anti-sunward) and $\mathbf{B_{SW}}$ is the upstream IMF.

In order to discuss the dependence of O^+ escaping ion flux on the upstream IMF direction, we calculate the cone angle, θ, which is the angle between the x-axis and the IMF direction. For each orbit we obtain θ_{in} by averaging over 5 minutes just before the spacecraft crosses the bow shock inbound and θ_{out} by averaging over for 5 minutes after the outbound crossing of the bow shock. Then we search for orbits belonging to one of the following two categories: 1) the perpendicular IMF case: orbits where the upstream IMF direction is perpendicular to the Venus-Sun line (x-axis) ($60° \leq \theta_{in}, \theta_{out} \leq 120°$) and 2) the parallel IMF case: orbits where the IMF direction is parallel (or anti-parallel) to the Venus-Sun line ($0° \leq \theta_{in}, \theta_{out} \leq 30°$ or $150° \leq \theta_{in}, \theta_{out} \leq 180°$). We consider only orbits that satisfy $\delta_{in}, \delta_{out} \leq 30°$ (δ_{in}, δ_{out} are standard deviations of θ_{in}, θ_{out}) and $|\theta_{in} - \theta_{out}| \leq 30°$, in order to remove orbits where the IMF direction fluctuates strongly or changes significantly during the period when VEX is inside the bow shock. In the period between 21 June, 2006 and 31 May, 2010, we found 167 perpendicular IMF cases and 82 parallel IMF cases. Note that many orbits are excluded from the current analysis in the parallel IMF case because IMF usually fluctuates and violates our criteria in δ_{in} and δ_{out}.

3. Observations

We integrate O^+ fluxes at the nightside of Venus for the two IMF cases. Using data of 167 perpendicular IMF cases and 82 parallel IMF cases, all the fluxes within the average bow shock [*Martinecz et al*., 2009] are assigned to spatial bins with the size 0.25 R_V × 0.25 R_V (1 R_V = 6050 km) in the VSE frame. Then the mean fluxes in each bin are calculated. We consider O^+ densities below 0.01 cm^{-3} as instrumental background and these data are regarded as no fluxes. We also include the O^+ flux that directs toward Venus, which is sometimes seen in our dataset. To make the escape flux statistically reliable, only bins that have been sampled at least three times are taken into account in the study.

Figure 1 shows maps of the binned fluxes for the perpendicular IMF case (a-c) and the parallel IMF case (d-f), and the number of measurements in the Y_{VSE}-Z_{VSE} plane for each IMF case (g-h). For the perpendicular IMF case, strong fluxes are seen in the center of the post terminator region in the X_{VSE}-Y_{VSE} plane (Figure 1a). Both in the Y_{VSE}-Z_{VSE} (Figure 1b) and X_{VSE}-Z_{VSE} (Figure 1c) planes, O^+ fluxes are concentrated at the poles where the magnetic field is expected to have large curvature. All these features are consistent with what was reported in *Masunaga et al*., [2011]. For the parallel IMF case, we instead see a relatively strong flux on the flank of Venus in the X_{VSE}-Y_{VSE} plane (Figure 1d). In the Y_{VSE}-Z_{VSE} plane, O^+ fluxes are not concentrated at the poles but rather randomly distributed over the Venus terminator (Figures 1e). Comparing Figure 1c and 1f, we note that also in the X_{VSE}-Z_{VSE} plane the flux distribution is different for perpendicular and parallel IMF cases. These features are also consistent with *Masunaga et al*., [2011].

From the binned flux maps we calculate an O^+ escape rate for the two IMF cases. We integrate all fluxes in the Y_{VSE}-Z_{VSE} plane that have been observed within the induced magnetoshere on the nightside, and obtain the total O^+ escape rates $F_\perp = (5.8 \pm 2.9) \times 10^{24}$ s^{-1} for the perpendicular IMF case and $F_\parallel = (4.9 \pm 2.2) \times 10^{24}$ s^{-1} for the parallel IMF case.

4. Discussion and Conclusion

The ratio of the escape rates is $F_\parallel/F_\perp \sim 0.8$ (0.3-2.4 with uncertainty). This result is compared with global hybrid simulations conducted by *Liu et al*. [2009] and *Johansson et al*. [2011]. Both authors investigated the plasma interactions between the solar (stellar) wind and an unmagnetized body changing the cone angle. *Liu et al*. [2009] compared O^+ escape rates at Venus between the perpendicular IMF case (cone angle 90˚) and the quasi-parallel IMF case (cone angle 36˚) using the same parameters (velocity, temperature and density) of the solar wind. The result showed that the escape rate for the parallel IMF case was slightly higher than that for the perpendicular IMF case ($F_\parallel/F_\perp = 1.3$) when the solar wind's density was normal ($n_{sw} = 14$ cm^{-3}). *Johansson et al*. [2011] performed a comparison of O^+ escape rates from a Venus-like planet caused by stellar wind interaction using different cone angles (90˚ for the perpendicular case and 10˚ for the parallel case). From their results of the hybrid runs, the ratio of the net O^+ ion escape rate between the parallel IMF case and the perpendicular IMF case is $F_\parallel/F_\perp = 0.73$. Even though they did not provide any information of uncertainty, both ratios from *Liu et al*. [2009] and *Johansson et al*. [2011] are not far from 1. The simulation ratios are well within the uncertainty range of our observation.

It is known that there are several mechanisms to accelerate O^+ ions from Venus. We cannot discuss the O^+ acceleration mechanism in detail for each IMF cases from the data shown here. However, the total O^+ outflow flux is determined by the sum of the flux of all outflow mechanisms. The different acceleration mechanisms must balance each other in order to keep the escape rate the same.

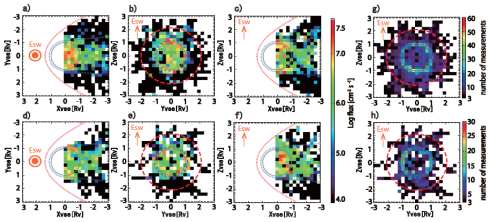

Figure 1: Maps of anti-sunward O^+ fluxes measured during a-c) the perpendicular IMF configuration and d-f) the parallel configuration and g-h) the number of measurements in the Y_{VSE}-Z_{VSE} plane for each case. The gray circle indicates the limb of Venus. White bins mean that there are less than 3 observations.

References

Barabash, S., et al. (2007), The Analyser of Space Plasmas and Energetic Atoms (ASPERA-4) for ther Venus Express mission, Planet. Space. Sci., 55, 1772-1792

Edberg, N. J. T., H. Nilsson, Y. Futaana, G. Stenberg, M. Lester, S. W. H. Cowley, J. G. Luhmann, T. R. McEnulty, H. J. Opgenoorth, A. Fedorov, S. Barabash, and T. L. Zhang (2011), Atmospheric erosion of Venus during stormy space weather, J. Geophys. Res., 116, A09308, doi:10.1029/2011JA016749

Futaana, Y., et al., Mars Express and Venus Express multi-point geoeffective observations of solar flare events in December 2006 (2008), Planet. Space Sci., 56, 873-880, doi:1016/j.pss.2007.10.014

Johansson. E. P. G., J. Mueller, and U. Motschmann (2011), Interplanetary magnetic field orientation and the magnetospheres of close in exoplanets, A&A, 525, A117, doi:10.1051/0004-6361/201014802

Liu, K., E. Kallio, R. Jarvinen, H. Lammer, H. I. M. Lichtenegger, Yu. N. Kulikov, N. Terada, T. L. Zhang, and P. Janhunen (2009), Hybrid simulations of the O^+ ion escape from Venus: Influence of the solar wind density and the IMF x component, Adv. Space Res., 43, 1436-1441, doi:10.1016/j.asr.2009.01.005

Luhmann, J. G., A. Fedorov, S. Barabash, E. Carlsson, Y. Futaana, T. L. Zhang, C. T. Russell, J. G, Lyon, S. A. Ledvina, and D. A. Brain (2008), Venus Express observations of atmospheric oxygen escape during the passage of several coronal mass ejections, J. Geophys. Res., 113, E00B04, doi:10.1029/2008JE003092

Martinectz, C., et al. (2009), Location of bow shock and ion composition boundaries at Venus - initial determinations from Venus Express ASPERA-4, J. Geophys. Res., 114, E00B30, doi:10.1029/2008JE003174

Masunaga, K., Y. Futaana, M. Yamauchi, S. Barabash, T. L. Zhang, A. Fedorov, N. Terada, and S. Okano (2011), O^+ outflow channels around Venus controlled by directions of the interplanetary magnetic field: Observations of high energy O^+ ions around the terminator, J. Geophys. Res., 116, A09326, doi:10.1029/2011JA016705

Taylor, Jr., H. A., H. C. Brinton, S, J. Bauer, R. E. Hartle, P. A. Cloutier, and R. E. Daniell, Jr. (1980), Global observations of the composition and dynamics of the ionosphere of Venus: Implications for the solar wind interaction, J. Geophys. Res., 85, 7765

Zhang, T. L., et al. (2006), Magnetic field investigation of the Venus plasma environment: Expected new results from Venus Express, Planet. Space Sci., 54, 1336

Zhang, T. L., et al. (2007), Little or no solar wind enters Venus' atmosphere at solar minimum, Nature, 450, 654-656, doi:10.1038/nature06026

Zhang, T. L., J. Du, Y. J. Ma, H. Lammaer, W. Baumjohann, C. Wang, and C. T. Russell (2009), Disappearing induced magnetosphere at Venus: Implications for close-in exoplanets, Geophys., Res., Lett., 36, L20203, doi:10.1029/2009GL04051